Reactions between M_n (M = Nb, Mo and n = 1, 2, 3, and 4) and N_2. A Density Functional Study

Attila Bérces,* Steven A. Mitchell, and Marek Z. Zgierski

Steacie Institute for Molecular Sciences, National Research Council, 100 Sussex Drive, Ottawa K1A 0R6, Canada

Received: March 11, 1998

Gradient-corrected density functional calculations were used to determine the most stable geometrical conformations and lowest electronic states of molybdenum and niobium atoms, dimers, trimers, and tetramers and their adducts with dinitrogen. The binding energies, geometries, and vibrational frequencies of the most stable conformations and electronic states are compared to experimental and theoretical results to the extent they are available. To interpret some of the peculiar features of related experimental data, we studied the ionization potential and electronic properties of MoN and NbN and the binding of more than one nitrogen molecule to metal trimers.

Introduction

The biological and chemical activation of dinitrogen has fascinated chemists for decades. A renewed interest in this subject has been fueled by the characterization of the active site of nitrogenase enzyme,[1] the natural catalyst of N−N bond activation, and consequent discoveries of inorganic complexes that break the N−N bond and reduce dinitrogen.[2] Researchers of our institute studied another aspect of nitrogen fixation, the reaction of N_2 with small metal clusters, to understand the fundamental driving forces of the cleavage of the N−N bond and to evaluate the similarities and differences between surface and cluster reactivities. Some experimental measurements of second-order rate coefficients of $M_x + N_2$ reactions have been done in our laboratory, which show a non-monotone trend of reactivity as a function of cluster size in the small (1−50 atoms) cluster size regime.[3]

To complement the experimental studies, we use quantum chemical calculations to gain an insight into the molecular orbital and steric interactions that govern reactivity. Methods based on density functional theory (DFT) in particular have been valuable tools to study a wide range of chemical systems including transition metal clusters. Thus, we carried out gradient-corrected DFT calculations to study various aspects of the $M_n + N_2$ reactions. In the present paper we report the structures of Nb_nN_2 and Mo_nN_2 clusters up to four metal atoms. Besides the main reaction products, we studied possible byproducts in order to interpret some of the peculiar features of the experimental data. The structures of M_2N_2 systems are discussed in a greater detail owing to their relevance to the ligand-supported binuclear, and larger, clusters.

Computational Details

The reported calculations employed the Amsterdam density functional (ADF 2.0.1) program system are derived from the work of Baerends et al.[4a] and vectorized by Ravenek.[4b] The numerical integration procedure was developed by teVelde[5] et al. The atomic orbitals on the metal atoms were described by an uncontracted triple-ζ STO basis set with a single polarization function, while a double-ζ single-polarized STO basis set was used for nitrogens.[6] A set of auxiliary[7] s, p, d, f, and g STO functions, centered on all nuclei, was used to fit the molecular density and represent the Coulomb and exchange potentials in each SCF cycle. We used the energy expression from the local density approximation[8a] in the Vosko−Wilk−Nusair parametrization augmented by gradient corrections to exchange[8b] of Becke and to correlation of Perdew,[8c] which was applied self-consistently.

Results and Discussion

Reactions of Metal Atoms with N_2. Tables 1 and 2 summarize the binding energies, geometries, and vibrational frequencies of the MoN_2 and NbN_2, respectively. We found linear end-on and planar side-on geometrical conformations as stable minima. The side-on bonded conformer of MoN_2 has the lowest energy in the $^5B_2$ state, which is bound only by 0.1 eV relative to the separated ground state (^7S) Mo atom and N_2. Thus, MoN_2 is only weakly bound and formed in a spin-forbidden reaction in accord with the experimental observation that Mo atom does not react with N_2.[9] On the other hand, the experimentally observed reactivity[10] of Nb with N_2 is reflected in the calculated potential that is barrierless and attractive on the $^6\Sigma^+$ surface with collinear geometry (Figure 1). The side-on NbN_2 is less stable than the linear structure, but it is still bound compared to the separate fragments.

Martinez and co-workers studied MoN_2 by gradient-corrected density functional methods in detail.[11] Their results on the stable structures and relative energies are in good qualitative agreement with ours. One notable difference is the relative energies of the lowest side-on and end-on bonded conformations. We found that the $^5B_1$ state of side-on conformation is more strongly bound ($\Delta E = -0.09$ eV) than the $^5\Pi$ state of the linear end-on conformation ($\Delta E = -0.03$ eV). On the other hand, Martinez et al. obtained the reverse relative stability of similarly weakly bound isomers ($\Delta E = -0.07$ and -0.15 eV, respectively). In addition to the structures described by Martinez et al., we found a transition state on the $^7\Pi$ surface that correlates to the ground state of Mo atom. The imaginary vibrational frequency corresponds to the degenerate bending coordinate, but we were unable to locate the bent structure since the potential energy surface is

S1089-5639(98)01452-2 CCC: $15.00 Published 1998 by the American Chemical Society
Published on Web 07/15/1998

TABLE 1: Binding Energies, Bond Lengths, and Vibrational Frequencies of MoN_2 Conformers[a]

state	$^3\Pi$	$^5\Pi$	$^7\Pi$	$^1A_1$	$^3B_1$	$^5B_1$
config.	end-on	end-on	end-on	side-on	side-on	side-on
bind. energy[b]	0.762	−0.032	0.005	0.308	0.477	−0.094
R_1 (N−N)	1.150	1.145	1.104	2.702	2.627	1.192
R_2 (Nb−N)	1.912	1.944	3.973	1.707	1.733	2.098
ν_1	310	280	i80	451	333	457
ν_1	486	463	48	914	716	474
ν_3	1891	1984	2371	1013	968	1724
z.p.e.	0.186	0.186	0.150	0.147	0.125	0.165

[a] Energies in eV distances in Å, and vibrational frequencies in cm^{-1}. [b] Binding energy relative to the sum of the energies of the isolated ground state (^7S) Mo atom and N_2 fragments.

TABLE 2: Binding Energies, Bond Lengths, and Vibrational Frequencies of NbN_2 Conformers[a]

state	$^2\Sigma^+$	$^4(\Pi, \Phi)$	$^6\Sigma^+$	$^2A_1$	$^4B_1$	$^4A_2$
config.	end-on	end-on	end-on	side-on	side-on	side-on
bind. energy[b]	0.497	-0.394	-1.439	-0.882	-0.803	-0.812
R_1 (N-N)	1.149	1.150	1.138	1.422	1.214	1.234
R_2 (Nb-N)	1.948	1.979	2.043	1.849	2.087	2.035
ν_1		306	287	431		
ν_1		405	406	708		
ν_3		1974	1974	1021		
z.p.e.		0.183	0.183	0.134		

[a] Energies in eV distances in Å, and vibrational frequencies in cm^{-1}. [b] Binding energy relative to the sum of the energies of the isolated ground state (^6D) Nb atom and N_2 fragments.

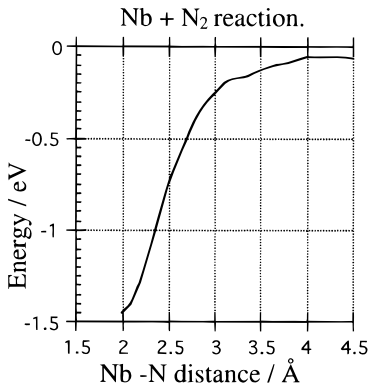

Figure 1. Energy diagram of Nb + N_2 reaction.

extremely flat. This structure has a very long Mo−N distance, and the energy is close to that of the separated fragments.

The variety of stable structures of N_2 adducts with transition metal atoms and clusters often arize from the stepwise breaking of the N−N bond. The side-on structures are suitable for the efficient charge transfer into the π^* and σ^* bonds of N_2 and manifest two distinct sets of geometries with partially broken (1.2−1.4 Å long) and fully broken (2.7 Å long) N−N bonds. The linear, end-on bonded structures do not provide efficient charge transfer into the antibonding orbitals of N_2 to significantly elongate or break the N−N bond. The reason why the linear structure can still be energetically very favorable is that metal−nitrogen bond can form without the cost of breaking or weakening the N−N bond.

The bond analysis developed by Ziegler and Rauk[12] provides further insight into the differences between the energetics of Nb and Mo interactions with N_2. Although this procedure is quite mathematical, the aim is to explain bonding in three simple terms: orbital interaction (ΔE_{el}), steric interaction (ΔE^0), and preparation (ΔE_{prep}) energies as shown in eq 1:

$$\Delta E_{binding} = \Delta E_{e1} + \Delta E^0 + \Delta E_{prep} \quad (1)$$

The total binding energy ($\Delta E_{binding}$) in our calculations represents the reaction energy of dinitrogen with a single atom. The term ΔE_{el} represents the main features of the common theory by Parr and Pearson in which the binding energy is related to the differences in electronegativity and hardness between interacting fragments.[13] The preparation energy, in this case, represents the stretching energy of the N−N bond to the appropriate distance in the MN_2 molecule from the equilibrium geometry of N_2.

The $^5\Pi$ state of MoN_2 and the $^6\Sigma^+$ state of NbN_2 in linear configuration are particularly appropriate for the comparison of the binding energy terms since the steric repulsion (4.2 eV) and the preparation energy (0.1 eV) are essentially the same in these two systems. Thus, the difference in the binding energies arises from the difference in the orbital interaction terms. The extra electron on the d shell of Mo atom yields a 1.2 eV more repulsive interaction between the filled σ orbital of N_2 and the d_{z^2} of Mo, compared to Nb. The combined interaction between the π and δ orbitals is the same for MoN_2 and NbN_2. Accordingly, the reduced σ repulsion is the main source of stronger binding in linear NbN_2. The 0.4 charge transferred into the N_2 fragment in MoN_2 is equally divided between the nitrogens, while the 0.3 charge transferred to N_2 in NbN_2 is more polarized and yields a 0.4 spin surplus on the distant N atom.

For the side-on isomers, we compared energy terms between analogous isomers with partially and fully broken N−N bonds. For these systems, it is more difficult to pinpoint a single energy term that is responsible for the stronger binding in NbN_2. The only consistent difference between MoN_2 and NbN_2 is the lowered repulsion between the σ of N_2 and the d_{z^2} of the metal in NbN_2 compared to MoN_2. However, the σ interaction is small in this conformation, and the rest of the contributions are inconsistent between MoN_2 and NbN_2. The combined σ^* and π^* interactions (both are b_1 symmetry in C_{2v}), for example, are 5.0 eV stronger in the ^1A_l state of MoN_2 than in the $^2B_1$ state of NbN_2 while, in the weakly bound analogues, the same interaction terms are in favor of the $^4A_2$ state of NbN_2 by 3.4 eV relative to the $^5B_1$ state of MoN_2.

Reactions of Metal Dimers with N_2. Metal dimers and larger clusters can yield adducts with N_2 in a large variety of geometrical conformations (Figure 2), and each conformation may exist in various spin states. M_2N_2 may also exist in unsymmetrical geometries or in T-shaped end-on bonded conformations, not shown in Figure 2. On the basis of our calculations, the most important conformations are the perpendicular and parallel bridging and the trans conformations. The linear M−N−N−M conformations can be found in ligand-supported inorganic complexes.[14] Blomberg et al.[15] studied the linear M−N−N−M and perpendicular bridging conformations of M_2N_2 systems with M = Ti, Y, and Zr. Although some of the characteristics of the ligand-supported clusters can be reproduced with the naked M_2N_2 systems, energetic preferences are highly altered by the coordinating ligands. We found that the linear M−N−N−M configuration is a high-energy and unlikely structure for the naked metal clusters in spite of its significance in inorganic chemistry. Energies, geometries, and vibrational frequencies of the most significant states and conformations of Mo_2N_2 and Nb_2N_2, based on our calculations, are listed in Tables 3 and 4, respectively.

The C_{2v} symmetry nonplanar perpendicular bridging conformation in the $^5A_2$ state is the ground state of Mo_2N_2 (structure **2**). The second lowest energy is the planar trans C_{2h} conformation in the ^1A_g state (structure **4.a**). The planar perpendicular

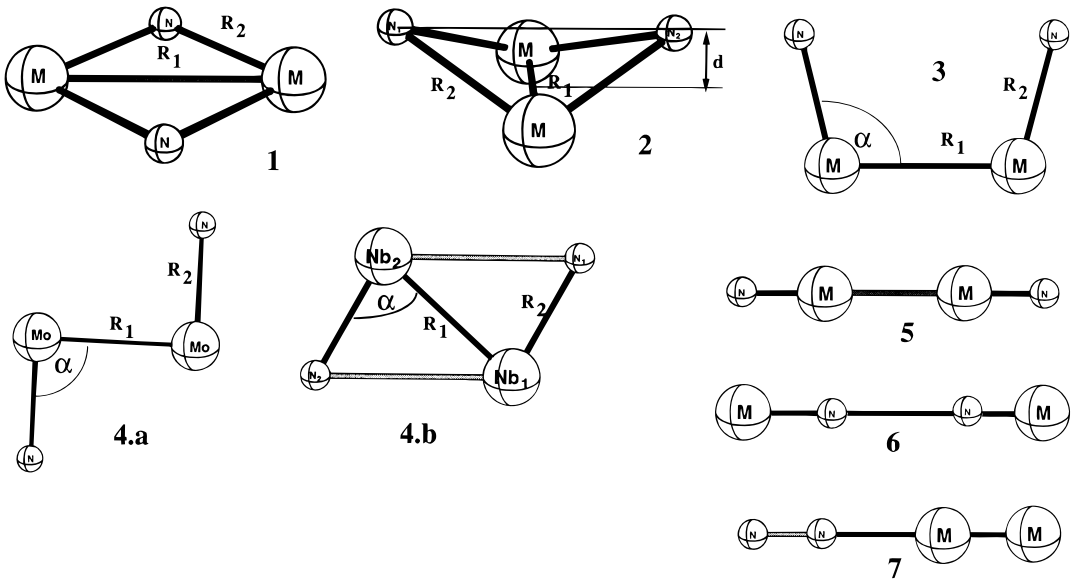

Figure 2. The structures of M_2N_2 conformers.

TABLE 3: Binding Energies, Geometries, and Vibrational Frequencies of Mo_2N_2 Conformers[a]

	perp. bridge					para. bridge		trans	
	D_{2h} $^1A_{1g}$	D_{2h} $^3B_{1u}$	D_{2h} $^5B_{1g}$	C_{2v} $^5A_2$	C_{2v} $^7B_2$	C_{2v} $^1A_1$	C_{2v} $^3B_1$	C_{2h} ^1A_g	C_{2h} ^3B_u
energy[b]	−28.423	−28.822	−28.415	−29.033	−28.917	−28.410	27.966	−29.008	−28.686
bind. energy[c]	0.306	−.093	0.314	−.304	−.188	0.320	0.763	−0.277	0.042
R_1 (Mo−Mo)	2.742	2.736	2.575	2.522	2.774	2.326	2.476	2.256	2.314
R_2 (Mo−N)	1.848	1.851	1.897	1.890	1.896	1.665	1.665	1.694	1.692
α						104.7	102.6	89.9	85.6
d				0.468	0.168				
ν_1	348 A_{1g}	352 A_{1g}	i1252 A_{1g}	266 A_1	205 A_1	139 A_2	96 A_2	143 B_u	115 B_u
ν_2	369 B_{1u}	154 B_{1u}	i272 B_{3u}	379 B_1	322 A_1	232 A_1	154 B_2	214 A_u	124 A_u
ν_3	486 B_{1g}	406 B_{1g}	33 B_{1u}	383 A_1	414 B_1	239 B_2	207 A_1	218 A_g	157 A_g
ν_4	669 B_{3u}	596 B_{3u}	354 B_{1g}	396 A_2	450 A_2	319 A_1	244 A_1	426 A_g	398 A_g
ν_5	731 B_{2u}	719 B_{2u}	441 A_{1g}	741 B_2	657 B_2	1044 A_1	1043 B_2	994 A_g	985 A_g
ν_6	869 A_{1g}	861 A_{1g}	714 B_{2u}	781 A_1	773 A_1	1057 B_2	1053 A_1	1021 B_u	1021 B_u
z.p.e.	0.215	0.191	0.096	0.183	0.175	0.188	0.173	0.187	0.174

[a] Energies in eV, distances in A, angles in deg, and vibrational frequencies in cm^{-1}. [b] Energy relative to sum of the energies of atoms with spherical charge densities. [c] Energy relative to sum of the ground state of Mo_2 and N_2 fragment energies without zero-point corrections. [d] Symmetry fables refer to an orientation in which the metal atoms are aligned with the x-axis and the N atoms accordingly in the C_{2v} and D_{2h} point groups.

TABLE 4: Binding Energies, Geometries, and Vibrational Frequencies of Nb_2N_2 Conformers[a]

	perp. bridge					para. bridge		trans	
	D_{2h} $^1A_{1g}$	D_{2h} $^3B_{3g}$	D_{2h} $^5B_{1g}$	C_{2v} $^1A_1$	C_{2v} $^3B_2$	C_{2v} $^1A_1$	C_{2v} $^3B_2$	C_{2h} ^1A_g	C_{2h} ^3A_g
energy[b]	−29.077	−29.617	−29.888	−29.630	−29.642	−27.055	−27.181	−28.426	−28.163
bind. energy[c]	−2.165	−2.705	−2.976	−2.718	−2.730	−.143	−0.270	−1.514	−1.251
R_1 (Nb−Nb)	2.725	2.737	2.815	2.275	2.718	2.632	2.699	2.250	2.355
R_2 (Nb−N)	1.885	1.889	1.909	1.965	1.893	1.695	1.699	1.745	1.754
α						102.3	104.7	76.2	73.2
d				0.6484	0.170				
ν_1	technical	i200 B_{1u}	259 B_{1u}	245 A_2	182 A_1	148 A_2	i121 A_2	i117 A_u	i186 A_u
ν_2	problem	355 A_{1g}	348 A_{1g}	372 A_1	337 A_2	177 A_1	149 A_1	250 B_u	186 B_u
ν_3		445 B_{1g}	371 B_{1g}	412 A_1	368 A_1	208 B_2	175 B_2	278 A_g	200 A_g
ν_4		570 B_{3u}	514 B_{3u}	505 B_1	565 B_1	209 A_1	187 A_1	416 A_g	342 A_g
ν_5		731 B_{2u}	691 B_{2u}	757 B_2	731 B_2	1020 B_2	1016 B_2	890 A_g	887 A_g
ν_6		827 A_{1g}	815 A_{1g}	806 A_1	825 A_1	1023 A_1	1018 A_1	943 B_u	911 B_u
z.p.e.		0.182	0.186	0.192	0.186	0.173	0.158	0.173	0.157

[a] Energies in eV, distances in Å, angles in deg, and vibrational frequencies in cm^{-1}. [b] Energy relative to sum of the energies of atoms with spherical charge densities. [c] Energy relative to sum of the ground state of N_{b2} and N_2 fragment energies without zero-point corrections. [d] Symmetry lables refer to an orientation in which the metal atoms are aligned with the *x*-axis and the N atoms accordingly in the C_{2v} and D_{2h} point groups.

bridging conformation (structure **1**) is lower in energy than the fragments but high compared to the lowest energy conformer. All parallel bridging conformations of Mo_2N_2 (structure **3**) are higher in energy than the separated Mo_2 and N_2. The most stable conformation of Mo_2N_2 is only 0.3 eV bound relative to the separated Mo_2 and N_2 fragments. In all conformations the nitrogen−nitrogen bond is broken; the distance between the nitrogens ranges between 2.6 and 4.1 Å. The Mo−Mo bond is also elongated by 0.3−0.7 Å compared to the metal dimer.

In contrast to Mo_2N_2, many geometrical conformations and electronic states of Nb_2N_2 are strongly bound (Table 4). The lowest energy $^5B_{1g}$ state of the planar perpendicular bridging

TABLE 5: Binding Energies, Geometries, and Vibrational Frequencies of the Precursor and Transition State of $Nb_2(N_2) \rightarrow Nb_2N_2$[a]

	precursor	transition state
energy[b]	−27.6416	−27.1326
bind. energy[c]	−0.7298	−0.2208
R_1 (Nb−Nb)	2.248	2.263
R_2 (Nb−N)	2.068	2.019
R_3 (N−N)	1.458	1.979
d	1.575	1.348
ν_1	95	iS23
ν_2	388	400
ν_3	402	435
ν_4	438	474
ν_5	625	669
ν_6	871	781
z.p.e.	0.175	0.171

[a] Energies in eV, distances in Å, and vibrational frequencies in cm^{-1}. [b] Energy relative to sum of the energies of atoms with spherical charge densities. [c] Binding energy relative to sum of the ground state of N_{b2} and N_2 fragment energies without zero-point corrections.

conformation with D_{2h} symmetry (structure **1**) is bound by 3.0 eV relative to the separated Nb_2 and N_2. In this structure, the N−N bond is broken, and the Nb−Nb bond is also elongated by 0.7 Å compared to the metal dimer. The $^3B_{3g}$ and the $^1A_{lg}$ states of the same (D_{2h}) conformation represent transition states between the nonplanar perpendicular bridging configuration in $^3B_1$ and $^1A_1$ electronic states, respectively. The corresponding nonplanar structures are the second and third lowest energy conformations. The $^3B_1$ state is similar in geometry to the lowest energy $^5B_{1g}$ structure with elongated Nb−Nb bond and broken N−N bond. On the other hand, the stable singlet bridging structure (C_{2v}) has a Nb−Nb bond of 2.28 Å, only slightly elongated compared to the 2.13 Å bond length in Nb_2. This structure, with a 0.65 Å distance between the centers of the Nb−Nb and N−N bonds, is strongly distorted from the planar position, and it has the longest Nb−N bond and the longest N−N distance of all perpendicular bridging configurations.

Both Mo_2N_2 and Nb_2N_2 prefer the perpendicular bridging configuration in a quintet state, but the most stable conformation of Nb_2N_2 is planar while that of Mo_2N_2 is nonplanar. The parallel bridging configuration (structure **3**) does not give energetically favorable states for either systems. There is a significant difference in the structures of Nb_2N_2 and Mo_2N_2 in the trans (C_{2h}) conformation (structures **4.a** and **4.b**). For the molybdenum system, the bond angle is very close to 90°, while it is over 100° for the niobium system. For Mo_2N_2, the trans conformation is one of the most stable conformations, while it is high energy for Nb_2N_2 compared to the most stable structures.

We recently reported a combined experimental and theoretical study of the precursor-mediated homolysis of N_2 in a reaction with Nb_2 on a singlet surface along with a detailed analysis of the orbital interactions.[16] Here, we only summarize the geometry, energy, and vibrational frequencies for the metastable minimum and the corresponding transition state in Table 5.

The reaction between dimers and N_2 may yield MN by fragmentation of M_2N_2, which may explain some peculiar features of previous experiments from our laboratory. In these measurements, the reaction products are detected by laser ionization mass spectrometry in which some products may go undetected if their ionization potential is too high. Thus, we calculated the fragmentation energetics of $M_2N_2 \rightarrow 2MN$ and the ionization potentials of MN. The calculated results for MoN and NbN and their cations are summarized in Tables 6 and 7, respectively. In accord with the expectation from qualitative

TABLE 6: Binding Energies, Geometries, and Dipole Moments of MoN and MoN^+[a]

	MoN $^2\Sigma^-$	MoN $^4\Sigma^-$	MoN^+ $^1\Sigma^+$	MoN^+ $^3\Sigma^-$
bind. energy[b]	−4.733	−5.5681	3.025	1.911
energy[c]	−12.463	−13.298	−4.706	−5.820
R	1.655	1.669	1.625	1.632
μ	2.601	3.228	3.793	3.851

[a] Energies in eV, distances in Å, and dipole moments in D. [b] Binding energy relative to sum of the ground state atomic energies. [c] Energy relative to sum of the energies of atoms with spherical charge densities.

TABLE 7: Binding Energies, Geometries, and Dipole Moments of NbN and NbN^+[a]

	NbN $^1\Sigma^+$	NbN $^3\Sigma^-$	NbN $^3\Delta$	NbN^+ $^2\Delta$	NbN^+ $^2\Sigma^+$	NbN^+ $^4\Sigma^-$
bind. energy[b]	−5.194	−6.153	−6.219	0.956	2.695	2.982
energy[c]	−11.446	−12.405	−12.471	−5.296	−3.557	−3.269
R	1.691	1.6959	1.6977	1.6597	1.6790	1.736
μ	5.96	6.03	3.74	4.72	3.38	3.73

[a] Energies in eV, distances in Å, and dipole moments in D. [b] Binding energy relative to sum of the ground-state atomic energies. [c] Energy relative to sum of the energies of atoms with spherical charge densities.

bonding arguments and previous generalized valence bond (GVB) calculations by Allison and Goddard,[17] MoN retains three unpaired electrons on δ_{xy}, $\delta_{x^2-y^2}$, and σ orbitals leading to the $^4\Sigma^-$ ground state. Our calculated bond length of 1.669 Å is slightly too long compared to the experimental value[18] of 1.636 Å and the calculated value of 1.603 Å obtained by Allison and Goddard. The calculated dipole moment of the ground state (3.23 D) is in accord with the experimental value[19] of 3.38(7) D and with the GVB calculated moment of 3.12 D. The dissociation energy of the ground state of MoN relative to the ^7S Mo and ^4S N atoms is 5.567 eV as opposed to the GVB results of 4.075 eV. We could not find an experimental value for the dissociation energy; therefore, it is difficult to find the reason for this disagreement. The ionization potential for $^4\Sigma^- \rightarrow {}^3\Sigma^-$ is 7.7305 eV. Consequently, MoN fragments cannot be detected in our experiments owing to their high ionization potential. It follows from Tables 3 and 6 that the fragmentation energy for the $Mo_2N_2 \rightarrow 2MoN$ process is 2.438 eV for the ground state of the lowest energy conformer of Mo_2N_2.

In agreement with experimental and other theoretical results,[20] we found that the ground state of NbN is $^3\Delta$. We also found that the $^3\Sigma^-$ state arising from the δ^2 configuration is very close in energy to the ground state, which previously has not been described. The experimental study of Azuma et al. concentrated on the states arising from the $\pi\delta$ configurations.[21] Our calculated equilibrium bond length (1.698 Å) is somewhat too long compared to the experimental value of 1.663 Å, while it is very close to the theoretical value (1.695 Å) obtained by multireference CI calculations. The calculated dipole moment (3.740 D) is somewhat larger than the experimental value of 3.26(6) D and again close to the calculated value of 3.65 D by high-level ab initio calculations. The ionization potential for the $^3\Delta \rightarrow {}^2\Delta$ transition is 7.175 eV. The fragmentation energy of the $Nb_2N_2 \rightarrow 2NbN$ process is 4.946 eV for the lowest energy conformer of Nb_2N_2.

Reactions of Metal Trimers with N_2. Before discussing the reaction products, let us first describe the metal trimers. The stable geometries of Nb_3 and Mo_3 molecules are listed in Tables 8 and 9, respectively. These molecules can adopt linear, D_{3h}, acute and obtuse C_{2v} and C_s symmetry structures. The lowest energy conformation of Mo_3 is an obtuse triangle close to C_{2v} symmetry with a spin multiplicity of 3. Although the geometry

TABLE 8: Relative Energies and Geometries of Mo_3[a]

symm.	D_{3h}	C_{2v} acute	C_s obtuse	C_s obtuse	C_{2v} acute	C_s obtuse	C_s obtuse
el. state	$^1A_{1g}$	$^1A_1$	$^1A'$	$^3A'$	$^2B_2$	$^5A'$	$^5A''$
energy[b]	−18.049	−18.147	−18.240	−18.726	−18.393	−18.652	−17.717
rel. energy	0.679	0.579	0.485	0.000	0.332	0.074	1.009
R_1	2.247	2.314	2.185	2.197	2.263	2.206	2.216
R_2		2.314	2.182	2.198	2.263	2.206	2.229
R_3		2.143	2.418	2.419	2.221	2.768	2.512

[a] Energies in eV, distances in Å, and vibrational frequencies in cm^{-1}. [b] Energy relative to sum of the energies of atoms with spherical charge densities.

TABLE 9: Relative Energies, Geometries, and Vibrational Frequencies of Nb_3[a]

symmetry	D_{3h}	C_s acute	C_s obtuse
el. state	$^2E''$	$^2A''$	$^4A'$
rel. energy	0.163	0.000	0.715
energy[b]	−17.673	−17.836	−17.121
R_1	2.335	2.382	2.349
R_2		2.382	2.349
R_3		2.255	2.462

[a] Energies in eV, distances in Å, and vibrational frequencies in cm^{-1}. [b] Energy relative to sum of the energies of atoms with spherical charge densities.

is close to C_{2v}, the electronic structure is only C_s symmetry. Upon symmetrization of the wave function and geometry optimization, an acute triangle is obtained, which is 0.32 eV above the lowest energy state. The obtuse triangle with $^5A'$ electronic state is only 0.07 eV higher in energy that the lowest conformation.

Goodwin and Salahub studied the small clusters of Nb atoms up to seven atoms based on local density functional theory.[22] In agreement with their results, we found the acute C_{2v} structure to have the lowest energy with a ground-state spin multiplicity of 2. Our optimized geometry with sides of 2.382, 2.382, and 2.255 Å is in good agreement with the LDA geometry found by Goodwin and Salahub with sides of 2.37, 2.37, and 2.26 Å. However, our geometry differs significantly from the optimized geometry of Goodwin and Salahub (2.32, 2.43, and 2.28 Å) obtained with gradient-corrected DFT methods. The C_{2v} structures were obtained by starting from an obtuse and an acute C_s symmetry starting point, both of which have converged to the same C_{2v} structure. The D_{3h} doublet state is only 0.14 eV higher than the lowest energy structure. The highest occupied molecular orbital is of degenerate E″ symmetry with only single electron occupations, which leads to the Jahn−Teller instability of the D_{3h} structure.

The structural alternatives for M_3N_2 clusters can be derived from the conformations for M_2N_2 by adding an extra metal atom to various positions. The most important conformations of M_3N_2 are shown in Figure 3. The binding energies, geometries, and vibrational frequencies of the lowest energy conformers and states of Mo_3N_2 and Nb_3N_2 are listed in Tables 10 and 11, respectively. The energetically most favorable structures of M_3N_2 are the trigonal bipyramidal (**8**), the square pyramidal (**9**), and the tetrahedron with a bridging N atom (**16**) structures, which all are related to the most stable perpendicular bridging conformations of the M_2N_2.

The preferred conformation of Mo_3N_2 is a tetrahedron bridged by a nitrogen atom (**16**) in the $^3A''$ state. This state is bound by 1.5 eV relative to the separated metal trimer and N_2. In this conformation, an additional Mo atom caps a face of two metals and one nitrogen of the nonplanar perpendicular bridging conformation of Mo_2N_2. The second lowest conformation is the square pyramidal structure (**9**) in the $^3A_2$ state with its energy

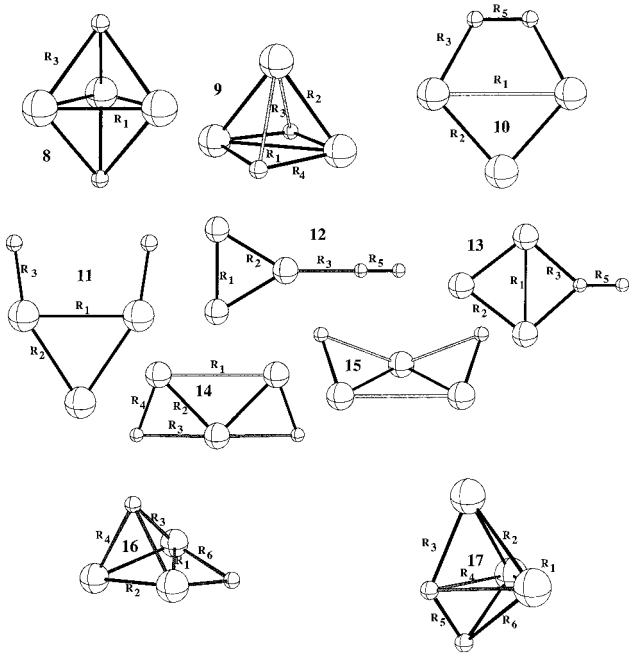

Figure 3. The structures of M_3N_2 conformers.

0.9 eV below that of the separated Mo_3 and N_2 molecules. The $^5B_2$ and $^1A_1$ states of the same conformations are only 0.15 and 0.25 eV above the energy of the $^3A_2$ state. The trigonal bipyramidal structure (**8**) with D_{3h} symmetry is energetically equivalent to the separated N_2 and Mo_3 fragments.

We previously characterized the gas-phase structure of Nb_3N_2 on the basis of zero electron kinetic energy photoelectron spectroscopy and density functional calculations.[23] The Nb_3N_2 cluster has a strong preference for the square pyramidal structure and prefers the low-spin electronic state. The $^2B_1$ state is 3.2 eV lower in energy than the separate N_2 and Nb_3 fragments. The energy of the trigonal bipyramidal structure is 1.5 eV above than that of the square pyramid. The second lowest energy conformer of Nb_3N_2 (structure **15**) has two nitrogen atoms in bridging position and slightly moved out of the plane of the metal trimer. The C_s symmetry structure is a transition state as indicated by the imaginary frequency. Following the mode of the imaginary frequency, the energy dropped by only less than 0.01 eV. Such distortions with negligible effect on the energy are very common in M_3A_2 molecules (M = transition metal, A = C, N) and related to the degenerate orbitals of the metal trimer. Owing to the flat potential surface, it is challenging to locate the minimum exactly. This conformation does not play a significant role in the reactivity of Nb_3 with N_2 owing to its high energy.

A linear transit calculation of the Nb_3 reaction with N_2 in a perpendicular bridging conformation, restricted to C_{2v} symmetry, showed the existence of a precursor and a transition state analogous to the dimer reaction in similar orientation. The

TABLE 10: Binding Energies, Geometries, and Vibrational Frequencies of Mo_3N_2 Conformers[a]

symm.	D_{3h}	C_{2v}	C_{2v}	C_{2v}	C_{2v}	C_{2v}	C_{2v}	C_{2v}	C_{2v}	C_s	C_s
	8	**9**	**9**	**9**	**10**	**11**	**12**	**13**	**14**	**15**	**16**
state	$^5A'$	$^3A_2$	$^1A_1$	$^5B_2$	$^3A_2$	$^3A_2$	$^5B_2$	$^3A_1$	$^3B_2$	$^5A'$	$^3A''$
energy[b]	−35.157	−36.055	−35.804	−35.904	−36.003	−32.378	−35.648	−35.932	−36.110	−36.030	−36.685
bind. energy[c]	−0.005	−0.903	−0.652	−0.752	−0.851	2.784	0.496	−0.780	−0.958	−0.878	−1.533
R_1 (Nb−Nb)	2.383	2.314	2.265	2.328	3.581	2.414	2.060	2.386	3.501	2.701	2.536
R_2 (Nb−Nb)		3.019	3.058	2.954	2.212	2.393	2.588	2.216	2.245	2.389	2.285
R_3 (Nb−N)	2.064	2.097	2.193	2.115	1.907	1.699	2.120	2.235	2.362	1.953	2.103
R_4 (Nb−N)			1.970	1.971	2.002				1.731	1.874	2.029
R_5 (N−N)	3.077	2.527	2.471	2.683	1.216	3.291	1.130	1.149			2.920
R_6 (Nb−N)											1.906
ν_1		76 b_1	198 b_1	i129 b_1						i146 a′	189 a′
ν_2		221 a_1	267 a_1	156 a_1						44 a″	202 a″
ν_3		245 a_1	294 b_2	275 b_2						154 a″	308 a′
ν_4		314 b_2	369 a_1	287 a_1						158 a′	318 a″
ν_5		420 a_1	417 a_1	347 a_1						265 a′	327 a′
ν_6		475 a_2	446 a_2	422 a_2						275 a″	389 a′
ν_7		527 b_1	550 b_1	437 b_1						483 a′	454 a″
ν_8		632 b_2	635 b_2	636 b_2						790 a″	696 a′
ν_9		761 a_1	735 a_1	654 a_1						926 a′	757 a′
z.p.e.		0.228	0.243	0.199						0.192	0.226

[a] Energies in eV, distances in Å, angles in deg, and vibrational frequencies in cm^{-1}. [b] Energy relative to sum of the energies of atoms with spherical charge densities. [c] Energy relative to sum of the ground state of Mo_3 and N_2 fragment energies without zero-point corrections. [d] Symmetry lables refer to an orientation in which the metal atoms are aligned with the *x*-axis and the N atoms accordingly in the C_{2v} and D_{2h} point groups.

TABLE 11: Binding Energies, Geometries, and Vibrational Frequencies of Nb_3N_2 Conformers[a]

symm.	D_{3h}	C_{2v}	C_{2v}	C_{2v}	C_{2v}	C_{2v}	C_s	C_s
state	$^2E'$	$^2B_1$	$^2A_2$	$^2A_1$	$^2B_2$	$^2A_2$	$^2A''$	$^2A'$
	8	**9**	**10**	**12**	**13**	**14**	**15**	**17**
energy[b]	−35.980	−37.488	−33.914	−34.191	−34.645	−36.192	−36.548	−35.533
bind. energy[c]	−1.717	−3.225						
R_1 (Nb−Nb)	2.395	2.356	3.066	2.288	2.747	3.293	3.010	2.330
R_2 (Nb−Nb)		2.855	2.312	2.329	2.265	2.368	2.418	2.425
R_3 (Nb−N)	2.130	2.371	1.972	2.243	2.079	2.250	2.123	2.101
R_4 (Nb−N)		1.970				1.780	1.813	2.262
R_5 (N−N)	3.241	2.712	1.275	1.124	1.194			1.320
R_6 (Nb−N)								2.165
ν_1		188 b1					i242 a″	
ν_2		257 a_1					98 a′	
ν_3		309 b_2					161 a″	
ν_4		310 a_1					194 a′	
ν_5		390 a_1					327 a′	
ν_6		449 a_2					351 a″	
ν_7		609 b_1					440 a′	
ν_8		667 b_2					839 a″	
ν_9		743 a_1					840 a′	
z.p.e.		0.243					0.202	

[a] Energies in eV, distances in Å, angles in deg, and vibrational frequencies in cm^{-1}. [b] Energy relative to sum of the energies of atoms with spherical charge densities. [c] Energy relative to sum of the ground state of Nb_3 and N_2 fragment energies without zero-point corrections. [d] Symmetry lables refer to an orientation in which the metal atoms are aligned with the *x*-axis and the N atoms accordingly in the C_{2v} and D_{2h} point groups.

corresponding structures are listed in Table 12. Additional imaginary vibrational frequencies are related to the C_{2v} symmetry restriction and correspond to metal trimer distortions. The 0.18 eV barrier, which separates the precursor from the product on the C_{2v} reaction path, may diminish if the symmetry restriction is removed. Since optimization on this extremely flat potential surface proved to be difficult, we did not locate these stationary points exactly. On the basis of these data, the reaction path of the dimer and the trimer follows qualitatively similar potential energy surfaces characterized by a precursor and a transition state. The barrier separating the precursor and the stable structure for the trimer reaction is significantly smaller compared to that of the dimer.

Our experimental reactivity study indicates that metal clusters with three or more atoms may react with more than one nitrogen molecule; in fact, metal trimers may take up to three nitrogen molecules. Therefore, we studied the structures and binding energies of the M_3N_6 clusters. We started the optimization with the three nitrogen molecules perpendicular bridging the three edges of the metal trimer but arrived at structures of Mo_3N_6 and Nb_3N_6 shown in Figure 4 after a significant reorganization. The binding energies and most important geometrical parameters of Mo_3N_6 and Nb_3N_6 are listed in Table 13. Both Mo_3N_6 and Nb_3N_6 can be described as a trigonal bipyramid core of Nb_3N_2 capped by nitrogen atoms on four faces. This arrangement allows stronger nitrogen−nitrogen interactions. The capping nitrogen atoms are only 1.4 Å away from the axial nitrogens, while the distance between capping nitrogens and metal is between 2.0 and 2.1 Å. Although Mo_3N_6 and Nb_3N_6 are structurally similar, they are energetically different. Nb_3N_6 is bound by 1.5 eV relative to the ground states of Nb_3 and three N_2 fragments. On the other hand, Mo_3N_6 is slightly higher in energy than the metal trimer and nitrogen fragments. This energetic difference is in accord with the observation that Nb_3N_6 is formed in the experiment, but Mo_3N_6 was not observed.

Metal Tetramer Reactions with N_2. In agreement with a previous study by Goodwin and Salahub, we found that the niobium tetramer adopts an ideal tetrahedron geometrical

TABLE 12: Binding Energies, Geometries, and Vibrational Frequencies of the Precursor and Transition State of $Nb_3(N_2) \rightarrow Nb_3N_2$ Restricted to C_{2v}[a]

	precursor	TS
state		
energy[b]	−34.5579	−34.3820
bind. energy[c]	−0.2951	−0.1192
R_1 (Nb−Nb)	2.816	2.787
R_2 (Nb−Nb)	2.408	2.417
R_3 (Nb−N)	2.005	1.917
R_4 (Nb−N)	3.236	3.161
R_5 (N−N)	1.596	1.917
ν_1	il35	i436
ν_2	283	i412
ν_3	294	i405
ν_4	332	il42
ν_5	381	280
ν_6	399	335
ν_7	547	397
ν_8	772	586
ν_9	807	727
z.p.e.	0.236	0.144

[a] Energies in eV, distances in Å, and vibrational frequencies in cm^{-1}. [b] Energy relative to sum of the energies of atoms with spherical charge densities. [c] Binding energy relative to sum of the ground state of Nb_2 and N_2 fragment energies without zero-point corrections.

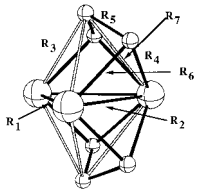

Figure 4. The structure of M_3N_6.

TABLE 13: Binding Energies and Geometries of Nb_3N_6 and Nb_3N_6[a]

symm.	C_{2v}	C_{2v}
state	$^3A_2$	$^2B_2$
energy[b]	−67.6698	−68.619
bind. energy[c]	0.335	−1.462
R_1 (Nb−Nb)	2.765	2.416
R_2 (Nb−Nb)	2.273	2.737
R_3 (Nb−N)	2.417	2.443
R_4 (Nb−N)	2.071	2.093
R_5 (N−N)	1.401	1.423
R_6 (Nb−N)	2.019	2.039
R_7 (Nb−N)	2.618	2.590

[a] Energies in eV, distances in Å, and angles in deg. [b] Energy relative to sum of the energies of atoms with spherical charge densities. [c] Energy relative to sum of the ground state of Nb_3 and 3 N_2 fragment energies without zero-point corrections.

configuration with sides of 2.480 Å in a singlet state. The tetramer of molybdenum prefers a D_{2d} structure with 2.239 Å bond length and 3.025 Å diagonal distance in a singlet state. The lowest quintet state of the ideal tetrahedron is 1.3 eV above the D_{2d} structure. The lowest energy conformation for both Mo_4N_2 and Nb_4N_2 can be derived from the tetrahedral metal core. In Mo_4N_2 one nitrogen caps one face and another nitrogen lies on an edge adjacent to the capped face, while both nitrogens of Nb_4N_2 cap one face each (Figure 5). The ground state of Mo_4N_2 is triplet, while that of Nb_4N_2 is singlet. The ground states of Mo_4N_2 and Nb_4N_2 are 1.41 and 2.54 eV bound compared to the metal tetramers and dinitrogen. In Mo_4N_2 only one of the N atoms binds to three Mo with bond lengths between 1.92 and 2.2 Å, and the other N atom binds only to two Mo atoms (1.86 and 1.99 Å). The conformation of Nb_4N_2 is more symmetrical where both nitrogen atoms bind to three niobium

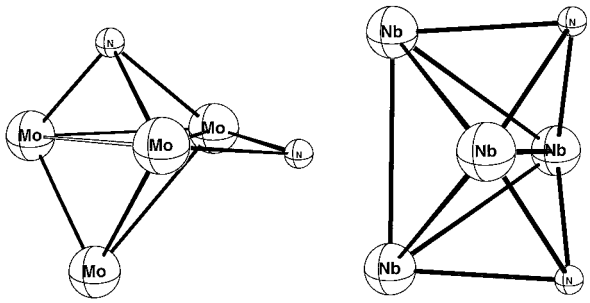

Figure 5. The most stable conformations of Mo_4N_2 and Nb_4N_2.

atoms. The geometry of the ground-state configuration of Nb_4N_2 is close to the C_s symmetry, with all NbN bonds close to 2.06 Å and two niobium and two nitrogen atoms in the symmetry plane.

Besides these structures, we considered the tetragonal pyramidal structure and its distorted variations, which were all higher in energy. Instead of describing each conformation by bond lengths, it is more appropriate for the M_4N_2 clusters to provide the Cartesian coordinate from which all internal coordinates can be derived. Such data is supplied in the Supporting Information. The Supporting Information includes some optimized geometries, vibrational frequencies, and relative energies of conformations of M_4N_2 clusters that have less significance and are not discussed in the text.

Conclusions

Density functional theory calculations of the energetics of molybdenum and niobium cluster reactions with nitrogen are consistent with the experimentally observed trends that niobium is more reactive than molybdenum. We found that the reduced repulsion between the filled σ orbital of N_2 and the dz^2 of Nb due to the lower d population of niobium is the only consistent difference between the orbital interactions of MoN_2 and NbN_2. This interaction term is responsible for stronger binding in the linear conformation of NbN_2 but has less significance in the side-on coordination. The calculations showed a large variety of possible geometrical conformations and electronic states for these clusters. The perpendicular bridging configuration preferred by M_2N_2 clusters is a structural motif of the most stable conformers of larger M_xN_2 clusters. In contrast to ligand-supported clusters, the linear MNNM conformation is energetically unfavorable for naked clusters. These calculations confirmed that MoN and NbN have high ionization potentials, which makes them undetectable in laser ionization mass spectrometry. The trimers of niobium follow a precursor-mediated reaction with N_2 similarly to the dimers; however, the barrier from the precursor to the transition state is smaller than that of the dimer. Trimers and larger clusters may react with more than 1 equiv of N_2, and niobium clusters are more likely to take up more nitrogen that molybdenum clusters.

Acknowledgment. This paper is issued as NRCC #40882.

Supporting Information Available: Optimized geometries, vibrational frequencies, and relative energies of conformations of M_4N_2 clusters (4 pages). Ordering and access information is given on any current masthead page.

References and Notes

(1) (a) Rees, D. C.; Chan, M. K.; Kim, J. *Adv. Inorg. Chem.* **1994**, *40*, 89. (b) Rees, D. C.; Kim, J.; Georgiadis, M. M.; Komiya, H.; Chirino, A. J.; Woo, D.; Schlessman, J.; Chan, M. K.; Joshua-Tor, L; Santillan, G.;

Chakrabarti, P.; Hsu, B. T. *ACS Symp. Ser.* **1993**, *535*, 170. (c) Kim, J.; Rees, D. C. *Biochemistry* **1994**, *33*, 389.

(2) (a) Fryzuk, M. D.; Love, J. B.; Rettig, S. J.; Young, V. C. *Science* **1997**, *275*, 1445.

(3) (a) Mitchell, S. A.; Lian, L.; Rayner, D. M.; Hackett P. *A. J. Chem. Phys.* **1995**, *103*, 5539. (b) Mitchell, S. A.; Lian, L.; Rayner, D. M.; Hackett, P. A. Unpublished.

(4) (a) Baerends, E. J.; Ellis, D. E.; Ros, P. *Chem. Phys.* **1973**, *2*, 41. (b) Ravenek, W. In *Algorithms and Applications on Vector and Parallel Computers*; te Riele, H. J. J., Dekker, Th. J.; van de Vorst, H. A. Eds.; Elsevier: Amsterdam, 1987.

(5) (a) Boerrigter, P. M.; te Velde, G.; Baerends, E. J. *Int. J. Quantum Chem.* **1988**, *33*, 87. (b) te Velde, G.; Baerends, E. J. *J. Comput. Phys.* **1992**, *99*, 84.

(6) (a) Snijders, G. J.; Baerends, E. J.; Vernooijs P. *At. Nucl. Data Tables* **1982**, *26*, 483. (b) Vernooijs, P.; Snijders, G. J.; Baerends, E. J. Slater Type Basis Functions for the Whole Periodic System; Internal report; Free University of Amsterdam: The Netherlands, 1981.

(7) Krijn, J.; Baerends, E. J. Fit functions in the HFS-method; Internal report (in Dutch); Free University of Amsterdam: The Netherlands, 1984.

(8) (a) Vosko, S. H.; Wilk, L.; Nusair, M. *Can. J. Phys.* **1980**, *58*, 1200. (b) Becke, A. D. *Phys. Rev.*, **1988**, *A38*, 2398. (c) Perdew, J. P. *Phys. Rev.* **1986**, *B33*, 8822; *B34*, 7046.

(9) (a) Mitchell, S. A.; Lian, L.; Rayner, D. M.; Hackett, P. A. *J. Chem. Phys.* **1995**, *103*, 5539. (b) Mitchell, S. A.; Rayner, D. M.; Bartlett, T.; Hackett, P. A. *J. Chem. Phys.* **1996**, *104*, 4012.

(10) McClean, R. E.; Campbell, M. L.; Kolsch, E. J. *J. Phys. Chem. A* **1997**, *101*, 3348.

(11) Martinez, A.; Köster, A. M.; Salahub, D. R. *J. Phys. Chem. A* **1997**, *101*, 1532.

(12) (a) Ziegler, T.; Rauk, A. *Theor. Chim. Acta* **1977**, *46*, 1. (b) Ziegler, T. General Energy Decomposition Scheme for the Study of Metal−Ligand Interactions in Complexes, Clusters and Solids, NATO ASI, in press. (c) Ziegler, T.; Rauk, A. *Inorg. Chem.* **1979**, *18*, 1558. (d) Ziegler, T.; Rauk, A. *Inorg. Chem.* **1979**, *18*, 1755.

(13) (a) Pearson, R. G. *Inorg. Chem.* **1988**, *27*, 734. (b) Parr, R. E.; Pearson, R. G. *J. Am. Chem. Soc.* **1983**, *105*, 7512.

(14) Cohen, J. D.; Mylvaganam, M.; Fryzuk, M. D.; Loehr, T. M. *J. Am. Chem. Soc.* **1994**, *116*, 9529.

(15) Blomberg, M. R. A.; Siegbahn, P. E. *J. Am. Chem. Soc.* **1993**, *115*, 6908.

(16) Bérces, A.; Hackett, P. A.; Lian, L.; Mitchell, S. A.; Rayner, D. M. *J. Chem. Phys.*, in press.

(17) Allison, J. N.; Goddard, W. A., III. *Chem. Phys. Lett.* **1983**, *81*, 263.

(18) Calculated from rotational constant B' of: Jung, K. Y.; Fletcher, D. A.; Steimle, T. C. *J. Mol. Spectrosc.* **1994**, *165*, 448.

(19) Fletcher, D. A.; Jung, K. Y.; Steimle, T. C. *J. Chem. Phys.* **1993**, *99*, 901.

(20) Fletcher, D. A.; Steimle, T. C.; Balasubramanian, K. *J. Chem. Phys.* **1993**, *99*, 9324.

(21) Azuma, Y.; Huang, G.; Lyne, M. P. J.; Merer, A. J.; Srdanov, V. I. *J. Chem. Phys.* **1994**, *100*, 4238.

(22) Goodwin, L.; Salahub, D. R. *Phys. Rev. A* **1993**, *47*, R774.

(23) Yang, D.-S.; Zgierski, M. Z.; Bérces, A.; Hackett, P. A.; Martinez, A.; Salahub, D. R. *Chem. Phys. Lett.* **1997**, *227*, 71−78.